Green enzymatic synthesis and processing of poly (*cis*-9,10-epoxy-18-hydroxyoctadecanoic acid) in supercritical carbon dioxide ($scCO_2$).

Domenico Sagnelli,[1] Ambra Vestri,[1] Silvio Curia,[1] Vincenzo Taresco,[1] Gabriella Santagata,[2] Mats K.G. Johansson,[3] Steven M. Howdle [1*]*

[1] University of Nottingham, School of Chemistry, University Park, Nottingham, NG7 2RD, UK

[2] Institute for Polymers, Composites and Biomaterials, National Council of Research, Via Campi Flegrei 34, 80078 Pozzuoli, Italy

[3] KTH Royal Institute of Technology, Department of Fibre & Polymer Technology, 10044 Stockholm, Stockholm

*corresponding author

KEYWORDS. Supercritical CO2, birch bark, cis-9,10-epoxy-18-hydroxyoctadecanoic acid, lipase, *Candida albicans lipase* B, enzymatic polymerisation, UV curing

Abstract

There is significant potential for industrial use of renewables for a wide range of materials demanded by society. Plants, trees and algae are increasingly attracting attention as sustainable sources for functionalised and polymerizable building blocks. In particular, the outer bark of the birch tree (*Betula pendula*) is a side stream of the forestry industry with so far very little utilisation besides energy recovery. It is composed of a macromolecular network, suberin, that could provide a renewable, low cost and

competitive resource. Within raw suberin is the potentially very useful multifunctional extract *cis*-9,10-epoxy-18-hydroxyoctadecanoic acid (CHA). Our drive has been to develop a green and sustainable synthetic strategy to CHA-based polyesters, by exploiting supercritical carbon dioxide ($scCO_2$) as a reaction medium and leveraging the regio- and chemo-selective properties of the biocatalyst Novozym 435 (Lipase B). Low temperature (35-55 ^oC) polycondensation in $scCO_2$ shows significant advantages compared to traditional polymerisation methods leading to reasonably high molecular weight polyesters. The mild synthetic conditions also preserve the valuable epoxy groups of the CHA which we show can be exploited by post-polymerisation functionalisation to create sustainable resins for bio-renewable coatings.

Introduction

The polymer industry is heavily reliant on time limited petrochemical reserves. Despite the fundamental role that polymers play in society, the vast majority of those are produced using monomers from petrochemical sources. In 2014 for example, just 1.7 million out of 300 million tons of globally manufactured polymers came from bioderived sources.[1] Therefore, interest in renewable resources as a replacement for fossil-based materials has increased considerably due to environmental concerns.[2–9] Sources of renewables ranging from trees, plants and algae could be exploited to extract novel functionalised molecules that can be converted in monomers in order to prepare novel renewable polymers.[10] These raw materials are not only of interest because of their abundance but also because they represent a unique opportunity to develop a circular economy in the polymeric field.[1,11]

Many naturally occurring polyesters act as structural components in plants and the monomer composition is complex and differs among plant species.[4] One interesting bio renewable source is the outer bark of the birch tree (*Betula pendula*). Birch bark is a by-product of the Swedish wood and paper industry

(estimated production: ~200,000 tonnes/year) in the Scandinavian region[12], and its major component is a macromolecular network called suberin.[2–5]

This network can be deconstructed through hydrolysis to liberate long carbon chain monomers with varying structures.[13,14] Although the suberin structure is not yet fully understood, the most abundant

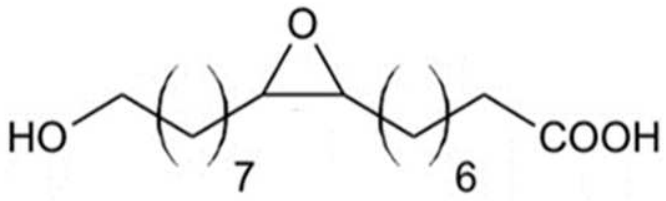

Scheme 1. *cis*-9,10-epoxy-18-hydroxyoctadecanoic acid (CHA) molecular structure highlighting the carboxyl and hydroxyl end groups and the epoxy ring moiety

monomer in this raw material is the Epoxy Fatty Acid *cis*-9,10-epoxy-18-hydroxyoctadecanoic acid (CHA – Scheme 1) which accounts for over 10% of the dry weight of the aliphatic content of suberin (multi) monomers (100 g/kg of dry birch bark). CHA is a unique polymerizable multifunctional molecule, which bears two terminal reactive groups: a carboxyl, a hydroxyl group, and an epoxy ring embedded along the alkyl chain. It should also be noted that most of the other aliphatic constituents of suberin are other ω-functional fatty acids with either a hydroxyl or a carboxylic acid as the ω-functionality[15]. This implies that even if the yield of the CHA monomer is less than 100%, the mixture can still be used to make polyesters as will be seen in the present study.

Epoxidized polymers are commonly used to form crosslinked networks because of the excellent mechanical strength, electrical insulation and thermal resistance of the final resins. Thus far, most of these polymers have been petroleum-derived and the industrial approaches to epoxidation of fatty acids

(FA) requires energy intensive processing.[16–19] There are examples of novel epoxy resins from lignin-based monomers but, although they provide elegant solutions, they do require use of fossil based and potentially toxic organic solvents for their synthesis .[18–20] Polymerization of naturally epoxidized fatty acids such as CHA and suberin/cutin has been an hot topic since early 2000[21] and the molecules extracted from suberin or cutin have been used to form polyesters through various methods. Initially, traditional methods were used ,for example acid catalysis for the synthesis of glycerol derivatives of cutin and suberin monomers.[21]Later greener approaches were tested in the search for mild reaction conditions for the synthesis of aliphatic polyesters.[12,19,22–26] Most notable examples use chemoenzymatic approaches for the synthesis of bio based polyester thermosets and resins.[12,25,26]These approaches use commercial lipase from Candida Albicans to polymerize in bulk or in organic solvents the EFA extracted from suberin/cutin

Accordingly CHA , because of its intrinsic chemical structure, could provide a “ready made” candidate for epoxy resins and smart coatings. In addition, chain length can be built up because CHA can be self-polymerised, through polycondensation yielding a linear epoxy-functionalised polyester.[2]

However, environmentally friendly bulk polymerisations show significant side reactions because of high viscosity. Carrying out the polymerisation in organic solvents may solve this problem, but then introduces issues around solvent removal, waste, and energy consumption. In recent years the use of supercritical carbon dioxide ($scCO_2$) as a reaction medium or temporary plasticiser for polymer synthesis and processing has increased steeply.[27–29] $ScCO_2$ has been exploited as a solvent for polymerisations,[30,31] as a foaming agent,[27,32] for precipitation of bio-macromolecules[33], for the extraction of compounds with pharmaceutical importance[34,35], particle formation and encapsulation of active ingredients.[36] The low critical point (31.1 °C and 7.4 MPa), its non-flammability, non-toxicity, and the low price and availability (driven by our use of fossil fuels) make $scCO_2$ a valuable and renewable alternative to conventional solvents.[37] $ScCO_2$ is a good solvent for many small molecules, but it is a poor solvent for most high-

molecular-weight polymers.[38] On the other hand, the solubility of $scCO_2$ into polymers can be high leading to significant swelling through penetration into the amorphous regions and increase of their free volume fraction. For this reason, $scCO_2$ can plasticise and effectively liquefy many polymers at temperatures below their glass transition temperature (T_g) and can lower melting point (T_m).[28,39,40] This viscosity reduction can be exploited to drive the polymerisation process towards completion, enabling monomer and oligomers to diffuse more rapidly.[41]

Polymerisation reactions have been studied extensively in $scCO_2$[31,42,43] with attention focussed on free radical polymerisations, but more recently enzyme catalysed polymerisations.[2,41] Similarly, the use of renewable natural monomers is a significant topic in modern polymer science.[1,44,45] Thus our aim has been to exploit this sustainable reaction medium, with mild reactions conditions, using bio-catalysis to create polymerizable building-blocks. Our target is high molecular weight linear polymers that preserve the epoxy groups and then to exploit these functionalised polymers for novel biomass-based epoxy resins via a thermal curing process. Two proof-of-concept applications are targeted: production of a xerogel-like material and a UV-crosslinkable resin both leading to 3D polymeric networks that might be considered greener alternative to conventional epoxy resins.

Materials and methods

Materials

The rawbirch bark was retrieved in the Stockholm region and dried and ground before monomer extraction. Novozym 435 (Lipase B from *Candida antarctica* immobilised on a macroporous acrylic resin) was kindly donated by Novozymes (Denmark) and dried under vacuum before use (0.1 bar at 25˚C for 24 h). Activated molecular sieves (4 Å, particle size 1.6 – 2.5 mm) were purchased from Fisher

Scientific (UK) and kept under vacuum (50 mbar at 50 °C). All other chemicals and solvents were purchased from Sigma-Aldrich (UK) and used as received. Supercritical Fluid Chromatography (SFC) grade 4.0 CO_2 (minimum purity 99.99%) was purchased from BOC Special Gases (UK) and used as received.

Methods and testseries

Bark hydrolysis and CHA extraction

The extraction of the epoxy fatty acid was performed by modifications to the protocol described by Nameer et al[46]. In particular, the residual soil and debris were removed from the bark by washing with water. Subsequently, the bark was vacuum dried (25 ºC) and ground into a fine powder using a coffee grinder (Krups - F203). A solution of 0.8M NaOH was set to reflux. Only when the temperature was stable at 100 ±1˚C was the powdered bark carefully poured in the solution (ratio 10:1 of base solution:bark). The hydrolysis reaction was stirred (300 rpm) and kept at steady conditions for 1h. To halt the reaction, the solution was rapidly cooled by immersion in an ice bath until the solution reached a temperature of 25℃. After centrifugation at 4500 rpm for 10 min the supernatant was collected. The supernatant was reduced to pH 5.8 using diluted glacial acetic acid to allow the precipitation of CHA. The supernatant was again centrifuged at 4500 rpm for 10 min and the pellet containing the isolated CHA was washed 3 times using MilliQ water (10:1) until the pH was set to neutrality (7.0). The extraction efficiency was calculated by weight and was 80 ±5% in line with previously published results, no difference was noted between small and large scale. The pellet was collected and vacuum dried at 25˚C. The relative purity after recrystallisation calculated using ^{1}H NMR was between 75-90%, depending on the nature of the raw material. The recrystallised monomer was analysed using 1H NMR to confirm that the epoxy groups (2.9 ppm) did not open during the hydrolysis or acidification process (Supplementary Figure 1).

^{1}H NMR ($CDCl_3$) δ: 1.2-1.8 (26 H, bm, -CH_2-), 2.3 (2H, t, J == 7.4 Hz, -$COCH_2$-), 2.9 (2H, bs, -CH- *cis*-epoxide), 3.6 (2H, t, J == 6.5 Hz, -CH_2OH).

^{13}C NMR ($CDCl_3$) δ: 178.54 (CO, C-1), 62.92 (-CH_2OH, C-18), 57.25 (-CH-, *cis*-epoxide, C-9 and C-10), 24.82-34.11 (14 C, -CH_2-).

Synthesis of poly(*cis*-9,10-epoxy-18-hydroxyoctadecanoic acid) (CHA)

In a typical procedure, the vacuum-dried monomer was placed in a 60 mL custom-made stainless-steel autoclave[33] in order to reach a final concentration of 5 mg/ml or 20 mg/ml in $scCO_2$. Molecular sieves (30% of the final weight of the monomer) and Novozym 435 (1.5 PLU/mg of monomer) were added and the autoclave was sealed and flushed with CO_2 at 2 bar for 5 min. After the flushing step, the temperature was set to 35 ˚C, 45˚C, 55˚C, or 85 ˚C and the pressure stabilised at 275 ±10 bar. At the end of the reaction (24h, 48h, 120h) poly (*cis*-9,10-epoxy-18-hydroxyoctadecanoic acid) (pCHA) was solubilised in tetrahydrofuran (THF) and precipitated in 10 volumes of ice-cold water. In parallel, bulkpolymerisations were performed for comparison purposes. The same separation/purification procedure was used. All reactions in the high pressure autoclave were stirred with a powerful magnetically-coupled mechanical stirrer.[47] The reproducibility of each polymerisation in scCO2 was tested in duplicate or triplicate, to establish the presence of polymer crosslinking.

^{1}H NMR (CDCl3) δ: 1.2−1.8 (26 H, bm, −CH2−), 2.3 (2H, t, J = 7.5 Hz, −COCH2−), 2.9 (2H, bs, −CH− *cis*-epoxide), 3.6 (t, J = 7.2 Hz, −CH2OH end group), 4.1 (2H, t, J = 6.5 Hz, −CH2O−).

^{13}C NMR (CDCl3) δ: 173.92 (CO, C-1), 64.46 (−CH2O−, C-18), 57.24 (−CH−, *cis*-epoxide, C-9 and C-10), 26.04−34.47 (14 C, −CH2−).

Nuclear Magnetic Resonance

Monomer purity and structural integrity of the polymer were determined using ^{1}H and ^{13}C NMR. All samples were analysed in deuterated chloroform ($CDCl_3$) using a Bruker Avance III 400 MHz spectrometer. The spectra were referenced to the solvent peak at $\delta = 7.28$ ppm corresponding to $CDCl_3$.

Fourier Transform Infrared Spectroscopy

Attenuated Total Reflection Fourier Transform Infrared (FTIR-ATR) spectroscopy was carried out on the surface of the samples by means of a Perkin-Elmer Spectrum 100 spectrometer (Waltham, USA), equipped with a Universal ATR diamond crystal sampling accessory. All the samples were analysed at room temperature. Spectra were recorded as an average of 32 scans in the range 4000–480 cm^{-1}, with a resolution of 4 cm^{-1}. No mathematical correction (e.g. smoothing) was done, while spectroscopic manipulation, such as baseline adjustment and normalisation, were performed using the Spectracalc software package OMNIC 9 (Thermo Fisher Scientific, Inc., MA, USA). Before testing, all samples were dried at RT 7.5 days

Size Exclusion Chromatography (SEC)

Molecular weight analysis was performed using an Agilent 1260 infinity multidetector GPC/SEC (Gel permeation chromatography /size exclusion chromatography) system equipped with a Wyatt Optilab with light scattering, UV and refractive index detectors. Columns consisted of 2 x Agilent PLGEL 5 μm Mixed D (7.5 mm X 300 mm) and a PLGEL 5 μm guard column (7.5 mm X 50 mm). THF was used as the eluent at an isocratic flow rate of 1 mL/min. The system was calibrated usingcalibration with narrow PMMA standards (range 1020000 to 540 $gmol^{-1}$).

Differential Scanning Calorimetry (DSC)

The samples were thermally investigated by using a Q2000 Tzero differential scanning calorimeter (DSC), TA Instrument (New Castle, DE, USA), equipped with a liquid nitrogen accessory for fast

cooling. The calorimeter was calibrated in temperature and energy using indium. Dry nitrogen was used as purge gas at a rate of 50 mL/min. Briefly, the dried samples (1.5~5 mg) were sealed inside Tzero DSC pan (TA Instruments, USA). DSC measurements were performed in a double heating run; the first one, occurring from -90 to 80 °C, at 10 °C/min, was performed to erase the thermal history of the samples. This scan was followed by a cooling ramp up to -90°C at a rate of 10°C/min. Finally, a second heating ramp up to 80 °C at 10°C/min was recorded. The last scan was repeated three times to give data confidence. The melting point (T_m) was taken as the maximum of the endothermic peak and the glass transition (T_g) temperature was evaluated as the inflection point of the heat flow change from the DSC thermograms.

Polymer curing thermal analysis

The curing of the polymer was examined using DSC. This experiment was designed to find out the curing temperature of the polymer studied. In particular, three scans were performed for every experiment. The samples were equilibrated at -20 ˚C and heated at a rate of 3˚C/min up to 250 ˚C. This scan was followed by a cooling scan at a rate of 3˚C/min down to -20 ˚C and finally another heating scan was performed (3˚C/min up to 250 ˚C). The first allowed us to find the onset and peak temperatures of the curing range. After the cooling phase the last heating scan was performed to find peaks associated with the curing reaction. The analyses were performed both with and without 1,6 hexanediamine as curing agent. Before the analysis the samples were premixed in batches overnight and subsequently weighted in the DSC pans.

Curing of poly(*cis*-9,10-epoxy-18-hydroxyoctadecanoic acid)

The production of the cured material was performed in Teflon cylindrical moulds (d=2 cm h=0.5 cm) at 150 ˚C for 1h. The polymer was cured alone or together with a curing agent (1,6 hexanediamine) at a

ratio of 1:1 (w:w). The monomer CHA with and without curing agent (1,6 hexanediamine) was used as control. The cured materials were formulated as described in Table 1 with or without the curing agent. In particular both low and high molecular weight pCHA polymer chains were used in the curing processes and these are subsequently referred to as pCHA-LMW and pCHA-HMW.

Table 1

Key components tested in curing process. The curing agent, when present, was in a ratio of 1:1 and the temperature of 150 (°C)

Starting Material	Molecular weight (Mn – $gmol^{-1}$)
pCHA-LMW	9000
pCHA-HMW	13000
CHA	314.5

Dynamic mechanical analysis (DMA)

DMA was used to determine the glass transition temperature (T_g) and moduli of the cured polymers (Table 2). Measurements were performed on a Triton Technologies DMA (now Mettler Toledo DMA) using the tension mode accessory and standard heating rate of 3 °C min^{-1} with a ramp from −50 to 100 °C. The experiments were performed on prototypes shaped as cantilever with a length of 10 mm and a width

of 2 to 3 mm. The T_g was estimated by comparing the derivative function of the storage modulus and the tan delta (tanδ) peak. Subsequently, the samples were treated with a controlled curing step at a rate of 10 ˚C /min in an interval between 100 and 250˚C. During the interval, an isotherm was kept constant for 5 min every 15 ˚C up to 250 ˚C. This step was performed to find out if the possible residual epoxides would react when the curing agent was consumed. After this step, the first heating gradient was performed again to evaluate any change in T_g and moduli.

Table 2

Materials tested using dynamic mechanical analysis. The curing agent, when present, was in a ratio of 1:1

Material	Molecular weight (Mn – $gmol^{-1}$)	Curing Temperature(°C)
Cured pCHA-LMW150	9000	150
Cured pCHA-LMW250	9000	150 and 250

Cured pCHA-HMW150	13000	150
Cured pCHA-HMW250	13000	150 and 250
Cured CHA	314.5	150

224

225 **$ScCO_2$ processing of cured materials and SEM analysis**

226 The cured materials were tested for pore formation and the effect of the MW of the polymer. In particular,
227 CHA, pCHA-LMW and pCHA-HMW cured materials were loaded in a porous and $scCO_2$ permeable
228 Teflon box which was sealed in the 60 mL base of a custom stainless-steel autoclave. The autoclave was
229 kept at a temperature of 60 ˚C and the pressure set to 275 bar for 1h. The pressure was released with a
230 rate of 5 bar/sec. The materials obtained were analysed using scanning electron microscopy (SEM).
231 Carbon tape (Agar) was placed on an SEM stub (Agar), the sample was then loaded, and sputter coated
232 for 90 seconds with an 8 nm thick coat of iridium. The imaging was performed under vacuum with a
233 typical accelerating voltage of 15 kV, using a Phillips XL30 (SEM). The pores and fibers were counted
234 and measured using ImageJ[48]. The number of features counted was approximately 50
235

236

237 **Crosslinking of CHA with UV**

238 Monomer solutions were prepared at 20 mg/mL concentration in THF with a photo-activator
239 (diphenyliodonium hexafluorophosphate - DPH) at three values of 0, 5 mmol%and 10 mmol%. Three

replicates were pipetted on glass plates. The samples were transferred to an argon glove box and irradiated with 2 UV lamps (2 × 15 W, 290 to 400 nm) for 20 min (Power density 10mW/cm^2).

Results and Discussion

Monomer solubility and high-temperature polymerisation

Using a custom-made view cell we determined that the CHA monomer (Supplementary Figure 2A) showed complete solubility in $scCO_2$ at 85 ˚C (Supplementary Figure 2B). However, a drop in solubility was observed when the temperature was lowered to 55 ˚C, 45 ˚C, and 35 ˚C and a phase separated CHA rich viscous fluid was observed (Supplementary Figure 2C) demonstrating also the very useful processing effect and lowering of T_m of the monomer by $scCO_2$ which might be exploited in polymerisation processes.

Lipase B extracted from *Candida Antarctica* and immobilised on acrylic beads (CALB - Novozym 435) was selected as mild catalyst for polymerisation of CHA. Previously published data suggested CALB is a well-suited catalyst for long-chain aliphatic ω-hydroxy acids polymerisation[2] and also green esterification in $scCO_2$.[49,50] For example, lipase efficiently catalysed the esterification of oleic acid with ethanol in $scCO_2$ at 40 ˚C[50] and the polycondensation of azelaic acid and 1,6-hexanediol in $scCO_2$ at 35 ℃.[49]

Comparison of Bulk and $scCO_2$ polymerisation at 85 ºC

Initially, the polymerisation reactions were carried out at relatively high temperature in order to assess the effect of $scCO_2$ and to align our results with the literature. The polymer was synthesised at 85 ˚C in $scCO_2$ (71% yield in weight) and in bulk (38% yield in weight), for comparison to conventional conditions (Table 3).

Table 3 *Molecular parameters of CHA in $scCO_2$ (yield 71%) and bulk (yield 38%) at 85 ºC detected by SEC at different polymerisation times (monomer concentration 5mg/ml).*

T=85 ºC	$scCO_2$			Bulk		
t(h)	Mn (gmolgmol^{-1})	Mw (gmolgmol^{-1})	Đ	Mn (gmolgmol^{-1})	Mw (gmolgmol^{-1})	Đ
1	1100	6500	5.9	1300	10100	7.8
3	4000	12000	3.0	2600	23700	9.1
5	5600	23000	4.1	2800	24900	8.9
24	18000	58700	3.3	1100	7100	6.4

The reactions were sampled over 24h (Figure 1) and the molecular weight increases rapidly during the first 5 hours of the reaction, both in $scCO_2$ and in bulk. However, for the bulk polymerisation the molecular weight appears to decrease significantly and after 24h the soluble material shows only M_n 1,100 gmolgmol^{-1}. It is most likely thatsignificant side reactions[46] of the epoxy ring led to crosslinking and insoluble materials. Since the insolubility of the polymer in any organic solvent generally indicates strongly the presence of some form of cross-linking it also explain the low apparent yield (38%) for the bulk strategy. By contrast high-molecular-weight pCHA is achieved in $scCO_2$ (Mn: 18000 gmolgmol^{-1}

282 and Mw: 58700 gmolgmol-1) after 24 h of reaction and the high yield and low dispersities indicate that

283 epoxide ring opening is likely minimised.

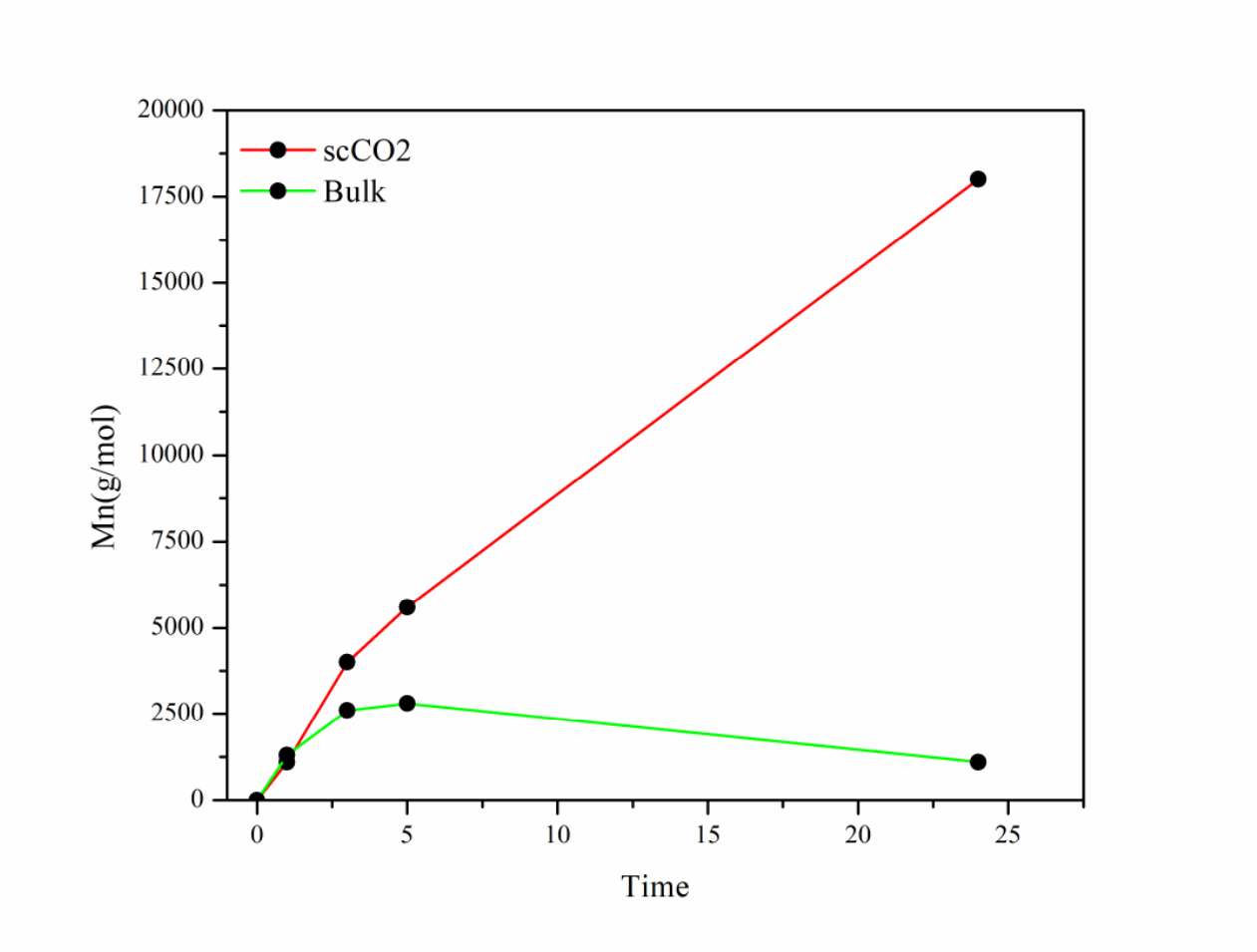

Figure 1. Polymerisation reactions of CHA in supercritical carbon dioxide and in bulk at 85 ˚C. The drop in molecular weight in the bulk reaction reflects the loss of soluble material through cross linking.

284 The reaction in $scCO_2$ gave much higher yields of high-molecular-weight materials; crosslinking side

285 reactions appear to be minimised. The soluble product shows four characteristic signals attributable to

286 pCHA in the ^{1}H NMR spectrum (Figure 2):

287

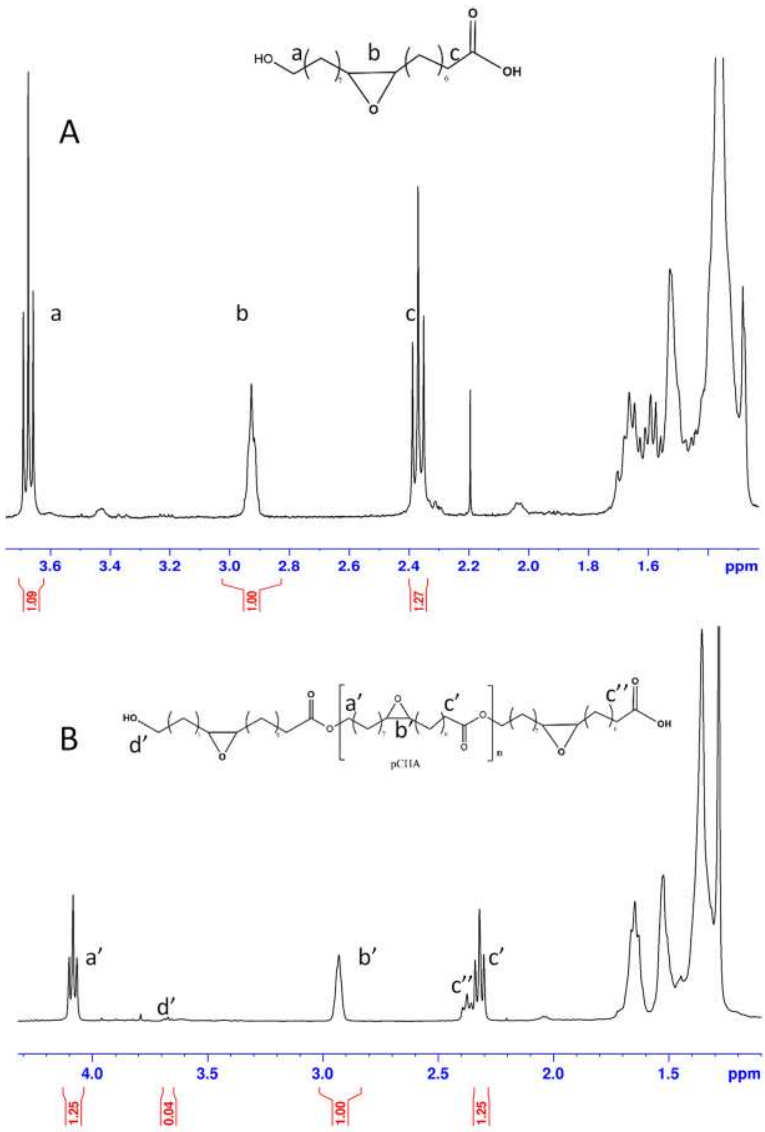

Figure 2. **A)** ^{1}H NMR spectrum of CHA in $CDCl_3$. a) 3.7 ppm (-CH_2-OH); b) 2.9 ppm (epoxy protons) and c) 2.3 ppm (-CH_2-COOH). **B)** ^{1}H NMR spectrum pCHA, in $CDCl_3$, synthesised in $scCO_2$ at 85 ^{o}C. The peak (b') at 2.9 ppm shows that the epoxy groups are preserved (integration 1:1 with peak a'), a' The broad peak between 1.2 and 1.7 ppm was assigned to the alkyl protons in the structure. d') 3.6 ppm (polymer end-group and monomer residues, -CH_2-OH);

Most notably, the ^{1}H NMR spectrum showed that the epoxy group is preserved after the polymerisation in $scCO_2$ and the peak areas of the protons belonging to the epoxy group (2.9 ppm) and the methylene protons of the ester carbonyl (2.3 ppm) have roughly a 1:1 ratio (Figure 2) confirming the expected stoichiometry. Moreover, the products were readily soluble in the common organic solvents used for routine analysis (chloroform or THF), thus confirming that little or no cross-linking due to ring opening of the epoxy group had occurred.

Low-temperature polymerisations of CHA in $scCO_2$

At lower temperature in $scCO_2$ the CHA monomer exists as a phase separated viscous oil (35-55 ^{o}C) (Supplementary Figure 2). Polymerisations under these conditions were carried out for 24h with a fixed monomer concentration of 5 mg/ml and led to lower molecular weights with Mn ranging from 7000 (35℃) to 2600 gmolgmol-1 (55 ˚C) (Table 4). A clear difference was noted when compared to 85℃ polymerization. In fact, at higher temperature (namely 85 °C) the monomer was fully solubilized leading to a faster growth of the polymer. Interestingly, very little cross-linked insoluble material was found in the product (by weight) and no branching in the ^{1}H NMR was detected in all the products and this is likely linked to the $scCO_2$ decreasing the viscosity of the plasticised reactants and facilitating the diffusion of monomers and oligomers very effectively.[41] Furthermore, at 35 ˚C the dispersity was much lower than at 85°C (1.3 to 3.3), possibly due to lower activity of the enzyme at that temperature. These results that it might well be worth optimising at lower temperatures.

Table 4.

Polymerisation in $scCO_2$ at different temperatures (35, 45 or 55°C) and reaction times 24, 48 or 120h. Mn, Mw and Đ of the pCHAs detected by SEC were reported.

Time(h)	T=35 °C			T=45 °C			T=55 °C		
	Mn (gmolgmol-1)	Mw (gmolgmol-1)	Đ	Mn (gmolgmol-1)	Mw (gmolgmol-1)	Đ	Mn (gmolgmol-1)	Mw (gmolgmol-1)	Đ
24	7000	9200	1.3	6700	11000	1.6	2600	3700	1.3
48	6500	18300	2.88						
120	6900	20400	2.9						

CHA polymerisation at 35 ºC: change in reaction time and effect on molecular weight

The reaction time was then increased up to 48h and 120 h (yield 63%), keeping the monomer concentration at 5 mg/ml (Table 4). This gave a significant increase in weight average molecular weight (Mw) but not number average molecular weight (Mn) which remained almost unchanged and furthermore did not match the reaction performed at 85ºC. We then increased the concentration of monomer (20 mg/ml) in addition to reaction time (48, 72 and 120 hours) and found that at 120h the molecular weight increased up to Mn 13000 gmolgmol-1 (Mw 54000 gmolgmol-1) (Table 5) demonstrating excellent potential for low temperature processing in $scCO_2$ as compared to literature.[51,52] There are also other possibilities for further process optimization. The products of the reactions could be improved in terms of polydispersity modulating the ratio between enzyme, monomer and solvent or by redesigning the reactor to be specifically used with enzymes. Clearly, our current results showed an increase in dispersity for longer reactions. A plausible explanation could be related to the ability of lipase in the presence of traces of water to hydrolyse polyesters and in our system this could be exacerbated if the molecular sieves become saturated. Because of size limitation of the autoclave, it was not possible to achieve meaningful results by increasing the amount molecular sieves in the reactor. We did observe that

the sieves were pulverised by the stirring during the reaction and this possibly could increase water traces likely driving unwanted hydrolysis and de-polymerisation.

Table 5.

Polymerisation in $scCO_2$ at a low reaction temperature (35°C) and high monomer concentration (20mg/ml). Mn, Mw and Đ of the pCHAs detected by SEC were reported

scCO2	**T=35C (20mg/ml)**		
Time(h)	Mn (gmolgmol-1)	Mw(gmolgmol-1)	Đ
24	9000	15000	1.6
48	11100	18000	1.6
120	13000	54000	4.2

Study of the thermal properties and curing of the polymers

After purification, the thermal properties of the polymers were characterised using DSC analysis. We focussed upon pCHA-LMW (M_n 9000 gmolgmol-1, M_w15000) and pCHA-HMW (M_n 13000 gmolgmol-1; M_w 54000) and found that the thermal properties of the samples do vary with molecular weight (Table

6). In particular, pCHA-HMW showed both higher melting (T_m) and glass transition temperature (T_g) when compared to pCHA-LMW (Table 6); in agreement with the data reported for propylene[53], poly-hydroxybutyrate [54], poly-lactic acid[55] and more recently for siloxanes and styrene polymers.[56,57]

To study the curing behaviour and the related thermal responses of these epoxy functionalised macromolecules, a series of DSC experiments were performed with and without added curing agent (1,6-hexanediamine) (1:1 w:w ratio -). For pCHA-HMW samples without curing agent an exergonic peak was detected in the first heating cycle with an onset at 142 ˚C, a maximum at around 198 ºC and a released energy of 32 J/g (Figure 3A). The exergonic event represents the epoxide groups crosslinking without a curing agent.[46] As might be expected, when the 1,6-hexanediamine was added the exergonic reaction occurred at a lower temperature with onset at 132 ˚C and the exergonic peak at 170 ˚C (Figure 3B). Interestingly, the energy released during the reaction was four times higher (130 J/g). These exergonic peaks can be associated with thermally activated crosslinking within the polymer chains, showing an increased yield of crosslinks when the curing agent was present. Similar results were recorded with the lower molecular weight material (9000 gmolgmol-1 - pCHA-LMW).

An exergonic peak in the DSC trace can be related to both chemical reaction or a recrystallisation event;[58] but recrystallisation can be ignored since this peak appears above the melting temperature. Furthermore, when the polymer was subjected to another heating cycle, no appreciable exergonic peak was detected (Figure 3C & D) making it clear that the peaks represent crosslinks formed in the polymer matrix. As further confirmation, when the curing agent is added to the mixture, a faster and more complete crosslink is achieved causing a higher energy release (compare Figure 3A and Figure 3B).

Table 6

T_g and T_m of low (pCHA-LMW) and high (pCHA-HMW) molecular weight pCHAs. The thermodynamic parameters were reported as calculated from the DSC traces

	T_g (˚C)	**T_m(˚C)**
pCHA-HMW	-42.0±1.6	31.4±0.2
pCHA-LMW	-60.7±2.2.	10.1±0.2

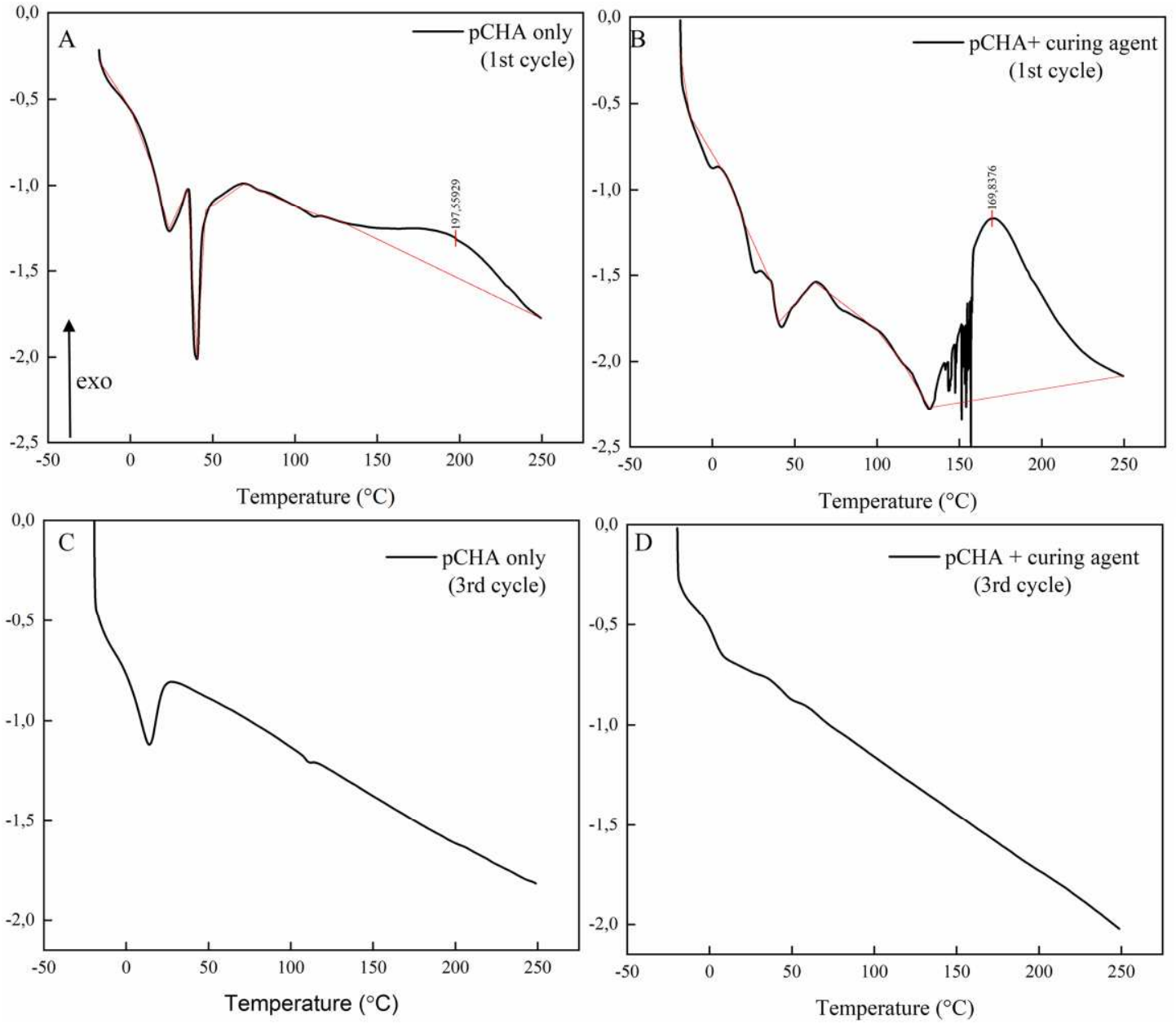

Figure 3. DSC profiles of thermal curing of the polymer. A) Curing of pCHA without curing agent. B) Curing of pCHA in the presence of the 1,6-hexanediamine crosslinking agent. C) and D) show the third cycle of the DSC traces where no exergonic peak is detected.

390

Preparation and analysis of the cured material

Once the thermal profiles were established by the DSC curing experiments, both pCHA-HMW and pCHA-LMW were used to produce cured samples. The polymers with and without the curing agent were placed in a cylindrical Teflon mould and the curing process was performed at 150℃ for one hour; this temperature chosen to be above the onset temperature for both samples (142 and 132℃) keeping the polymers in the same processing conditions. After the curing process, the materials were left to cool on ice and peeled off. Part of the peeled material was cured again at a higher temperature (250℃) to determine if any residual epoxide groups were present and would react.

As the cross-linked polymers were insoluble in common organic solvents (Supplementary Figure 4), the cured materials were analysed in their solid state by FTIR to show that all the 1,6-hexanediamine was consumed during the reaction (Figure 4). No significant differences were detected between the FTIR traces of cured pCHA-HMW and pCHA-LMW (Supplementary Figure 5).

Following the curing process by monitoring the epoxy bands is not ideal because of restriction of the specific group response. In fact, in the far and medium IR the epoxide rings show only low-intensity transitions. The main peaks associated with the epoxy ring signal (815 – 950 cm^{-1}) appear in the so-called "fingerprint region" (500-1400 cm^{-1}) thatthat can cover the band of interest. Despite the low intensity of the epoxy group, the non-cured material showed characteristic peaks around 846 cm^{-1} that flattens in the cured materials (Supplementary Figure 5), hinting at the disappearance of the epoxy ring on the polymer.[59,60] The changes in bands associated with the curing agent were also analysed since these are very reliable for crosslink analysis.[60] In particular, the peak related to symmetric and asymmetric stretching of the primary amine of the curing agent (3160 and 3330 cm^{-1}) was shown to disappear in both materials (Figure 4 – red circles). The cured materials showed only a broad signal around 3315 cm^{-1} possibly related to the stretch –OH group formed after the epoxy ring was opened.

415 It was possible to crosscheck the efficiency of the reaction by comparing the absorptions in the region
416 1650-1500 cm^{-1} (Figure 4), where primary and secondary amines are very easy to detect. In particular, it
417 is possible to detect the primary and secondary amine signal comparing cured and uncured pCHA. In
418 fact, new peaks are detected at 1646 and 1550 cm^{-1} in the cured material profile (green circle). No

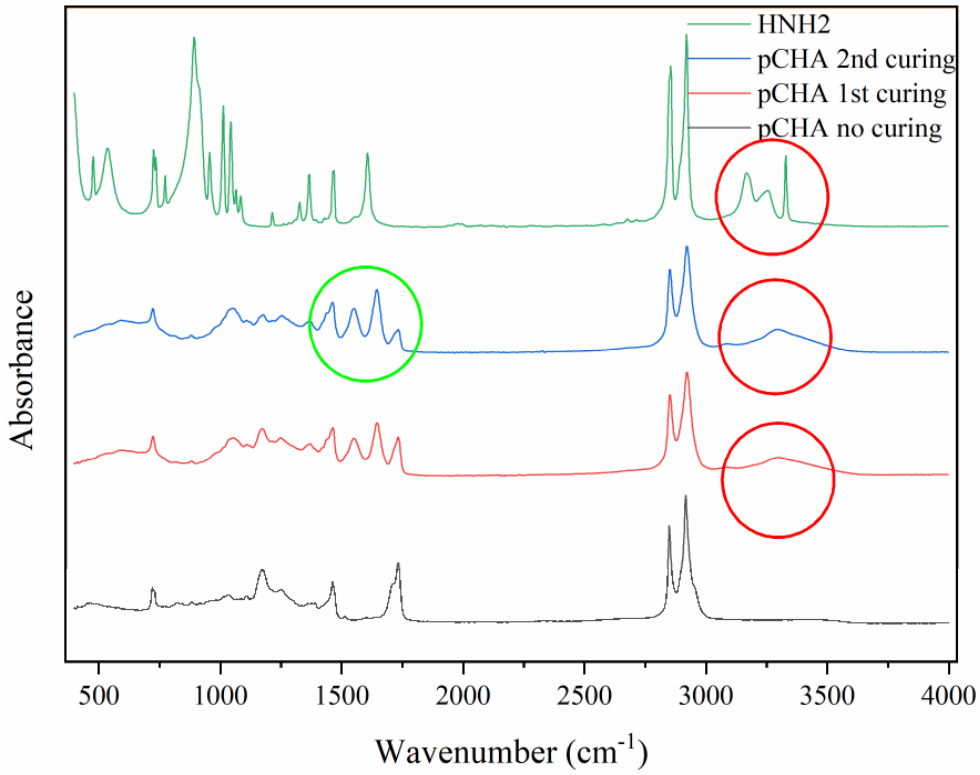

Figure 4. FTIR of cured materials and controls. The red circle indicates the presence of the N-H bands associated with the 1,6 hexanediamine primary amine (RNH2). The green circle shows the region representing the N-C bands of secondary and tertiary amines formed after the crosslinking reaction.

significant difference was assessed between the materials cured at either 150 or 250 ^{o}C indicating that the diamine was completely consumed.

Study of the thermo-mechanical analysis of the cured materials.

The viscoelastic and thermal properties of the cured materials were analysed using dynamic mechanical analysis (DMA) to yield the storage modulus (G') representing the elastic contribution of the material resistance to the deformation and the loss modulus (G'') related to the viscous response.[61]

The materials were analysed under varying temperature (dynamic mode) allowing us to identify the mechanical relaxation region corresponding to tan δ (glass transition temperature –T_g).

The materials processed at 150 °C without curing agent were wax-like materials and did not show any significant stiffness at room temperature. For this reason, it was not possible to obtain data using DMA.

When the curing agent was used, the crosslinked pCHA-LMW (pCHA-LMW150) showed both a bi-modal tan δ curve (Figure 5A), with a main transition at around T=23,5 ℃, which may be representative of the glass transition temperature, and a second broad feature between 30 and 65 ℃ (Figure 5A second curing step was performed by heating the samples up to 250 ℃ (pCHA-LMW250). This was to determine the presence and reactivity of any residual epoxides which would be revealed by changes in the tan δ profile. Changes were clearly observed with two distinct peaks both at higher temperature, circa 32 and 62 ^{o}C respectively, than the previous T_g (Figure 5B). It is well-known that the Tg of a cured polymeric system is mainly affected by molecular rigidity and cross-linking density. Therefore, for the same material a higher Tg could be indicative of higher degree of crosslinking[62]. These results show that post-curing effects were present during the second curing phase, hinting that the first curing step did not achieve full conversion of all the epoxy groups even if, as shown in the FTIR, the curing agent appeared to be fully consumed[63] (Figure 4 - red circle). Our hypothesis is that the uncompleted crosslinking may give rise to the broad feature because of an uneven distribution of the network formed and due to the complexity of the system broad range of crosslinked structures can be formed.[64]

Concerning the storage modulus, differences were observed between the materials. In fact, the material cured at 150 °C shows a modulus higher than of the material processed at 250 °C only before its main transition (*circa* 23.5 °C) was reached. In fact, when the temperature surpasses the Tg of pCHA-LMW150, the G' of the two materials abruptly swap. This behaviour is evident, when the storage moduli are compared on a log-scale. (Figure 6) A relatively small drop of G' before the rubbery plateau for the pCHA-LMW250 sample, may indicate a higher crosslinking density compared to the less crosslinked pCHA-LMW150 (Figure 6).

Crosslinked pCHA-HMW showed similar thermal behaviour. When cured at 150°C (pCHA-HMW150) (Supplementary Figure 6) showed a broad T_g at around 22 ℃ and a wide-relaxation region. But after the second curing at 250 ^{o}C (pCHA-HMW250), the Tg increased up to circa 38 ˚C. The storage modulus of crosslinked pCHA-HMW did not change as abruptly as pCHA-LMW after the second curing and this is most probably because of the higher Mw and limited mobility. As observed for pCHA-LMW, a shift of the G' was evident indicating a higher crosslinking density for the materials cured at higher temperature.

461

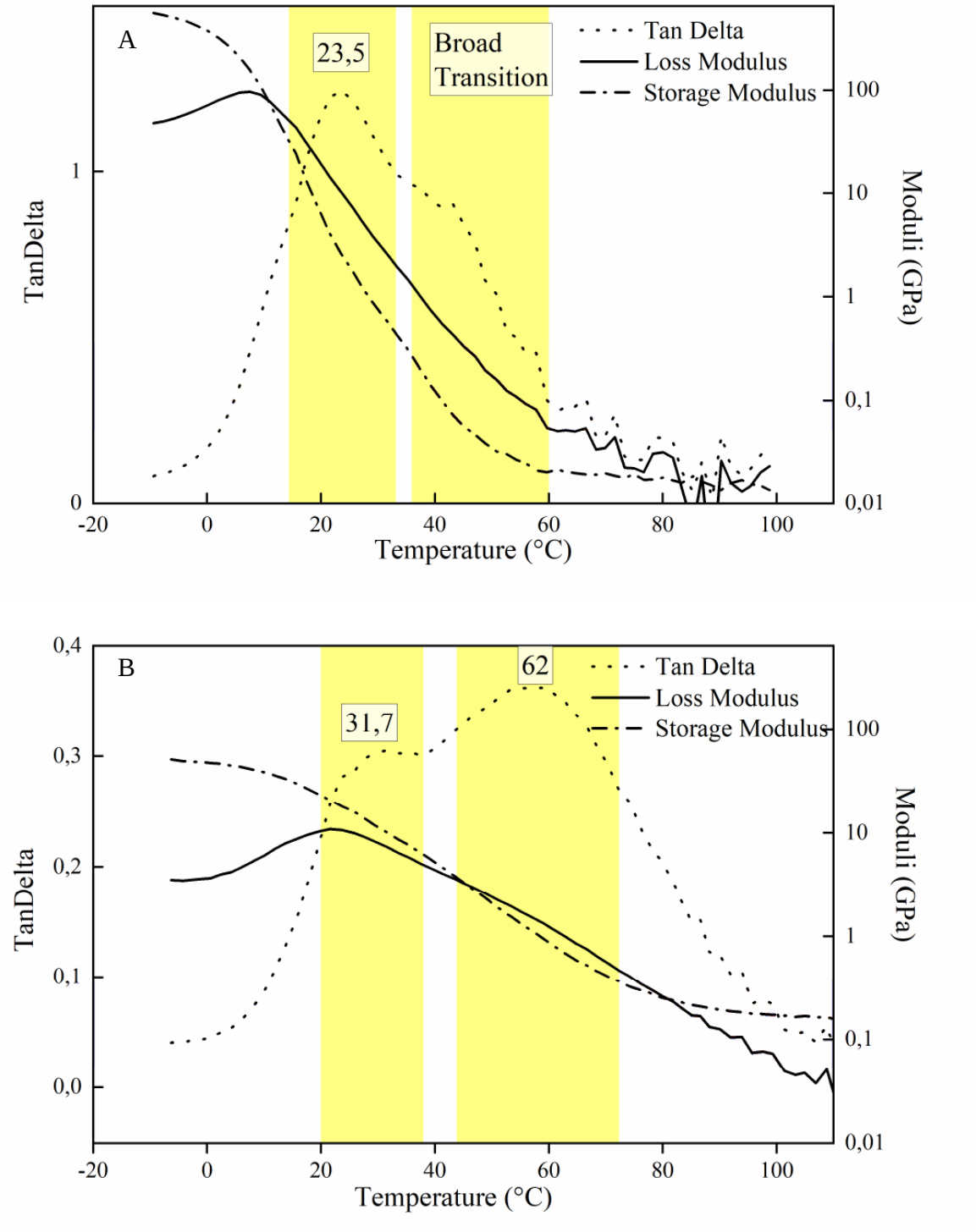

Figure 5 Dynamic mechanical analysis of pCHA-LMW cured materials. A) pCHA-LMW150 Cured material at 150℃ B) pCHA-HMW250 Material cured firstly at 150 ˚C and then at 250℃

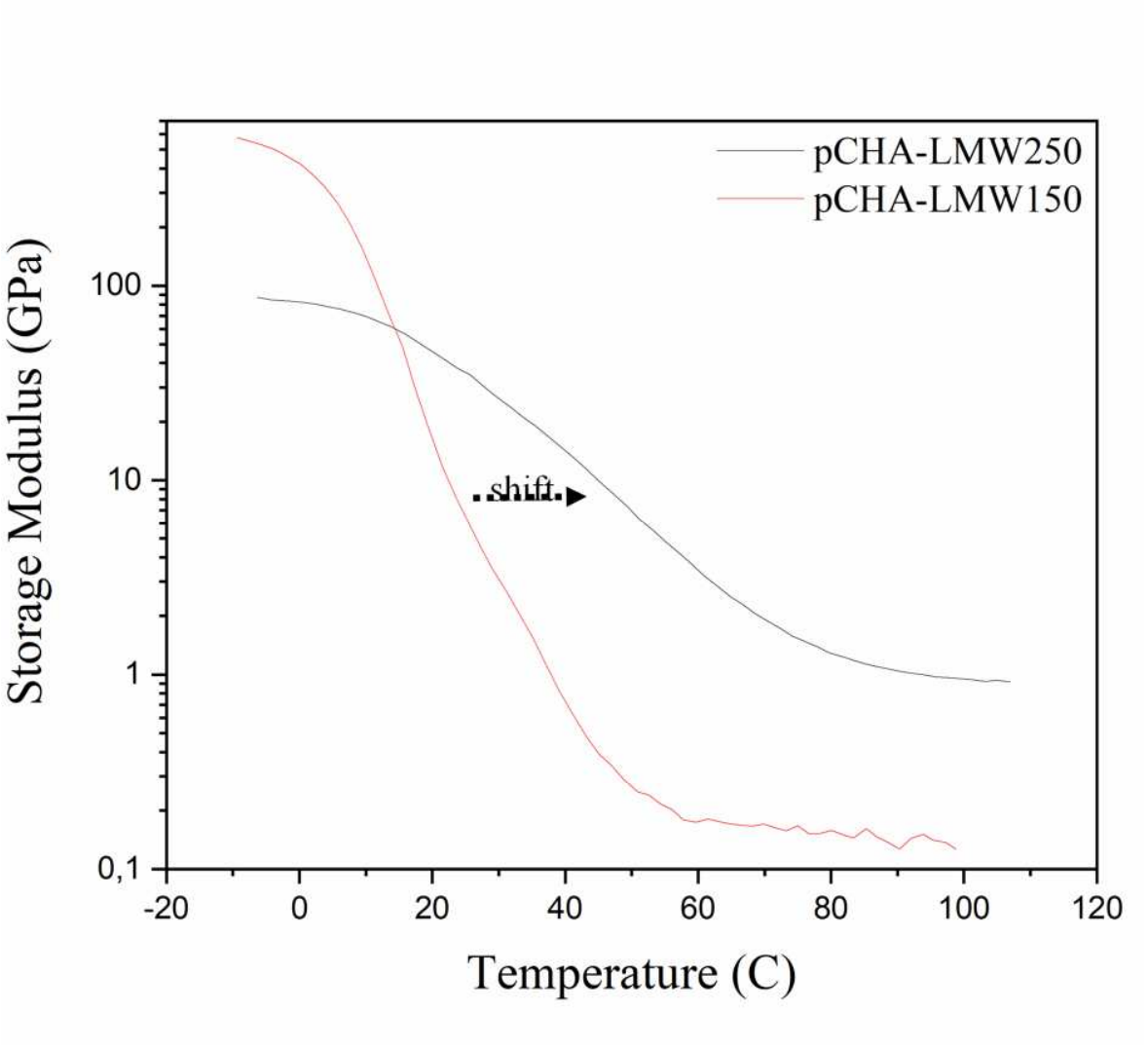

Figure 6. Comparison between the G' of pCHA-LMW cured at 150 ºC (red line) and 250 ºC (black line). The material cured at 150 °C show a higher modulus, the difference is evident when the temperature in the DMA is below the Tg of pCHA-LMW150. The shift of the G' likely indicates a higher crosslinking density.

Proof-of-concept: Xerogel-like material production without the use of traditional solvents

The surface morphology of the cured materials was analysed by scanning electron microscopy (SEM) before and after treatment with $scCO_2$ (Figure 7). These experiments were performed to prove that CHA based materials have potential for green post-synthesis processing. In this case we show the possibility to use a solvent-free process to produce xerogel-like materials which could be used in biomedical applications.[65] These materials are normally produced by swelling a crosslinked polymer with water to form a hydrogel.[65] The water is substituted with a more volatile solvent that is evaporated with a freeze-drier or in $scCO_2$ to form a sponge-like material. The major difference with the traditional protocol is thatat here we show a route that can be achieved in the complete absence of solvents to produce a highly porous material. In fact, the pCHA-HMW and pCHA-LMW cured materials were used immediately after they had been peeled from the teflon-mould.

As a control, the pure monomer was cured (CHA-cured) under similar conditions. As expected, all the materials prior the $scCO_2$ treatment showed a pore-free surface. Materials based on low and high MWW polymers were compared with the control showing a rougher surface (Supplementary Figure 7). In particular, for pCHA-LMW it is possible to see features resembling fiber-like (d==0.560 µm) and lumplump-like (d== 2,9±0.5µm) structures (Supplementary Figure 7D). These structures are possibly due to the post-crosslinking shrinkage and assembly.

After $scCO_2$ treatment, pCHA-LMW (Figure 7B) showed a very clear xerogel-like appearance with micro pores (2 µm to 50 µm) distributed across its entire volume (Figure 8B). CHA-cured samples did not show very effective pore formation (Figure 7D).

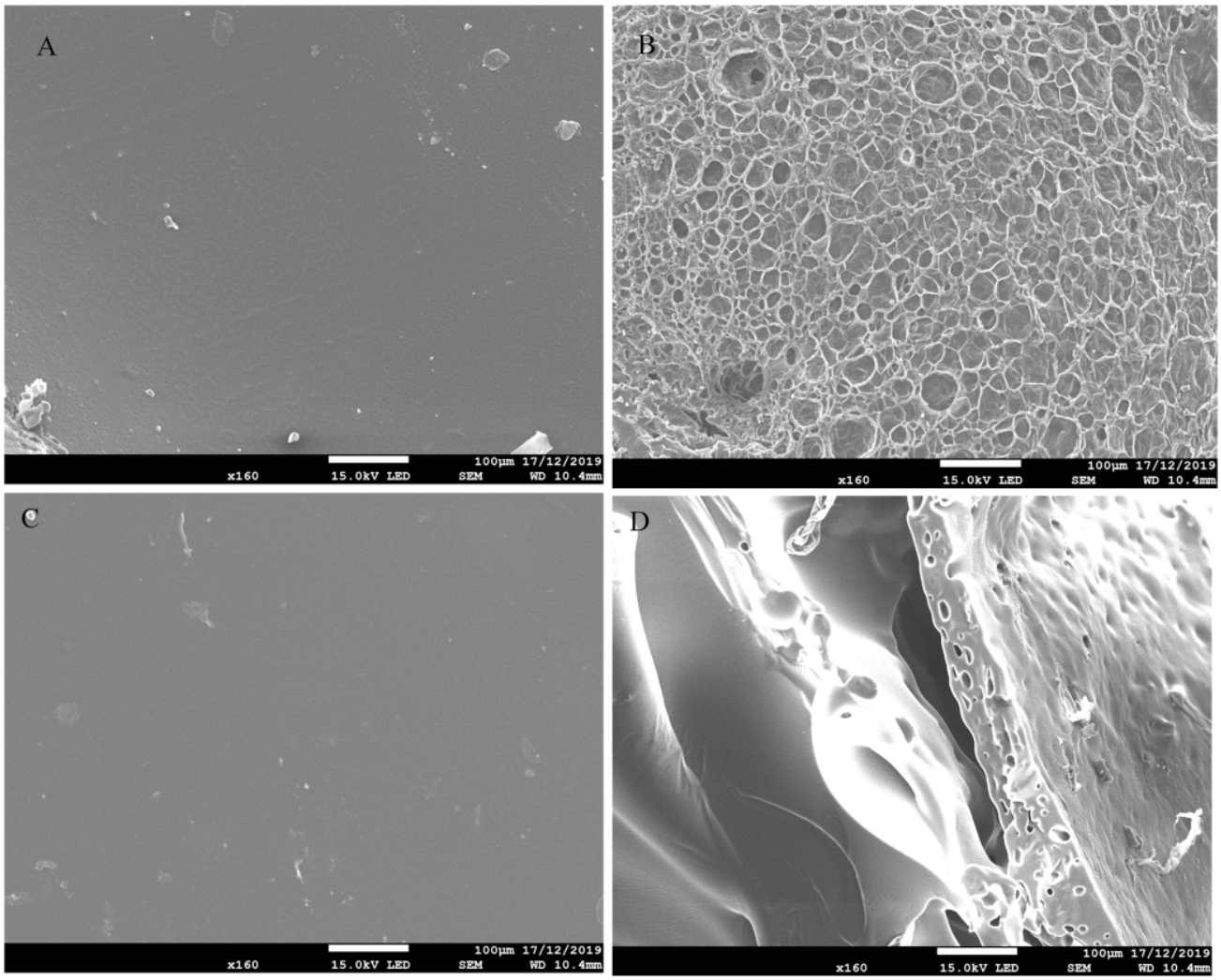

Figure 7. SEM images of the surfaces of pCHA-LMW and control and : A) and B) represent the pCHA-LMW material. A) before the scCO2 treatment and B) after the release of $scCO_2$. C) and D) represent the monomer cured (CHA-cured). C) before the $scCO_2$ treatment and D) after the release of $scCO_2$.

Proof-of-concept: UV crosslinking of CHA

With the aim to show that our material could be used as cross-linkable green ink potentially for 3D printing applications, we tested the crosslinking behaviour of CHA under UV light. Photo-curing is one

of the most effective routes to rapid transformation of multifunctional monomer resins to cross-linked polymer networks.[66] Photo-curing has been widely studied and applied in many industrial applications over the past decade exhibiting high efficiency, high-speed, low energy consumption and low activation-temperature.[67]

Here, UV-crosslinking was performed on the CHA monomer in presence of 5 mmol% and 10 mmol% of diphenyliodonium hexafluorophosphate (DPH), a cationic and photoacid initiator previously used for fast curing of epoxy resins.[68] CHA alone and in the presence of DPH was irradiated with UV light for 20 minutes at room temperature and analysed by FTIR. The region between 815 and 950 cm^{-1} is normally associated with oxirane (epoxy ring) vibrations[59,60] and here we could detect significant modifications related to epoxide vibrational modes following UV curing of CHA monomer without (cCHA) and with DPH (DPH5-cCHA, DPH10-cCHA). Specifically, small intensity vibrations around 794, 824 and 846 cm^{-1} (are attributed to the C-O-C stretching modes of oxirane rings whereas absorption bands at 890, 900 and 916 cm^{-1} (Supplementary Figure 8 Bottom) are ascribed to C-O stretching. Essentially, from the analysis of the spectra (Figure 8A) it was possible to observe a significant modification of the oxirane vibration modes which indicates ring opening. For example, the decrease and broadening of the peaks in DPH5-cCHA, likely indicate partial ring opening followed by crosslinking reaction. Comparison between the spectra of crosslinked samples and curing agent did not show any overlapping (Figure 8A). Furthermore, similar behaviour was noted comparing the oxirane region of irradiated samples with the diamine crosslinked CHA. Interestingly, when increasing the concentration of DPH seems that the curing efficiency decrease. In fact, the peaks at 890, 900 & 916 cm-1 are more visible for DPH10 cured sample than for the DPH5.

The analysis of the spectra of DPH10-cCHA samples at high frequencies of the FTIR spectra showed a broadening of the hydroxyl group vibration mode at around 3465 cm^{-1} as previously observed when the CHA was crosslinked with diamine (Figure 8B and Figure 4). In pure non-irradiated CHA spectra the

hydroxyl groups showed a sharp peak at 3465 cm^{-1} (Figure 4). A comparison of the entire spectrum is present in supplementary material (Supplementary Figure 8 Top):

514

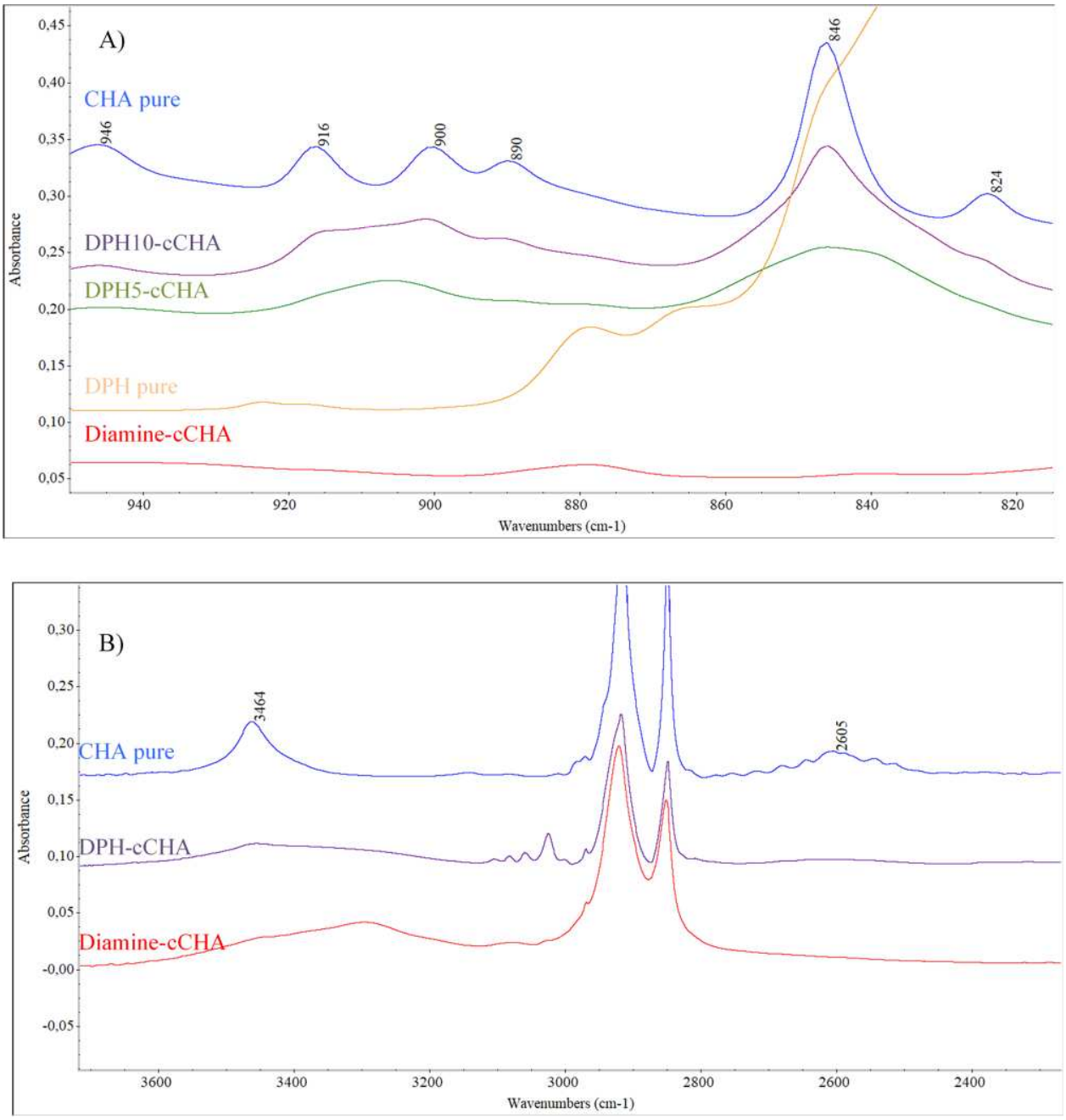

Figure 8. FTIR-ATR spectra range A) from 820 to 940 cm^{-1} and B) from 2400 to 3600 cm^{-1} of pure CHA (blue), UV catalysed cCHA: DPH1010-cCHA (purple) and DPH5-cCHA (green), Catalyst spectra (orange), hexendiamine catalysed cCHA(red).

Conclusion

We demonstrate facile polymerisation of a renewable monomer CHA extracted from birch bark. We utilise CaLB as catalyst and $scCO_2$ as a solvent and processing medium to ensure the retention of the epoxy groups; confirmed by ^{1}H NMR after extraction and polymerisation. The advantageous combination of CaLB and $scCO_2$ allowed for use of low temperature sustainable reaction conditions and avoided side reactions possibly present when the polymerisation was performed in bulk. Interestingly, high molecular weight polymers were obtained (pCHA Mn 18000 gmol-1) demonstrating that the biomass-based monomers can be utilised to create useful, functionalised polymers. The thermal properties of synthesised polymers were explored with DSC utilised to perform curing tests with and without curing agent, showing that pCHA has a relatively low curing temperature (150℃) in presence of curing agent. Additionally, we showed also that the CHA monomer was reactive under UV light giving rise to the possibility to produce novel biomass derived and green epoxy resins and coatings.

Acknowledgement and Funding resources

The research leading to these results has received funding from the Danish council for independent research, grant number 7026-00060B and People Programme (Marie Curie Actions) of the European Union's Seventh Framework Programme FP7/2007-2013/under REA grants agreement No. [289253]. We thank Richard Wilson, Martin Dellar and Mark Guyler (University of Nottingham) for the technical input with the high-pressure equipment. Furthermore, we would like to thank Ninfa Rangel Pedersen and Novozymes to have kindly supported the project providing the CalB.

REFERENCES

(1) Zhu, Y.; Romain, C.; Williams, C. K. Sustainable Polymers from Renewable Resources. *Nature* **2016**, *540* (7633), 354–362. https://doi.org/10.1038/nature21001.

(2) Olsson, A.; Lindström, M.; Iversen, T. Lipase-Catalyzed Synthesis of an Epoxy-Functionalized Polyester from the Suberin Monomer Cis-9,10-Epoxy-18-Hydroxyoctadecanoic Acid. *Biomacromolecules* **2007**, *8* (2), 757–760. https://doi.org/10.1021/bm060965w.

(3) Ivenrsen, T.; Nilsson, H.; Olsson, A. A Method for Separating from Suberin and/or Cutin Containing Plants, a Solid and/or Oil Fraction Enriched in Cis-9,10- Epoxy-18-Hydroxyoctadecanoic Acid. **2010**, 1–12.

(4) Pinto, P. C. R. O.; Sousa, A. F.; Silvestre, A. J. D.; Neto, C. P.; Gandini, A.; Eckerman, C.; Holmbom, B. Quercus Suber and Betula Pendula Outer Barks as Renewable Sources of Oleochemicals: A Comparative Study. *Ind. Crops Prod.* **2009**, *29* (1), 126–132. https://doi.org/10.1016/j.indcrop.2008.04.015.

(5) Gandini, A.; Pascoal Neto, C.; Silvestre, A. J. D. Suberin: A Promising Renewable Resource for Novel Macromolecular Materials. *Prog. Polym. Sci.* **2006**, *31* (10), 878–892. https://doi.org/10.1016/j.progpolymsci.2006.07.004.

(6) Montanari, U.; Cocchi, D.; Brugo, T. M.; Pollicino, A.; Taresco, V.; Romero Fernandez, M.; Moore, J. C.; Sagnelli, D.; Paradisi, F.; Zucchelli, A.; Howdle, S. M.; Gualandi, C. Functionalisable Epoxy-Rich Electrospun Fibres Based on Renewable Terpene for Multi-Purpose Applications. *Polymers (Basel).* **2021**, *13* (11). https://doi.org/10.3390/polym13111804.

(7) Xu, J.; Sagnelli, D.; Faisal, M.; Perzon, A.; Taresco, V.; Mais, M.; Giosafatto, C. V. L.; Hebelstrup, K. H.; Ulvskov, P.; Jørgensen, B.; Chen, L.; Howdle, S. M.; Blennow, A. Amylose/Cellulose Nanofiber Composites for All-Natural, Fully Biodegradable and Flexible Bioplastics. *Carbohydr. Polym.* **2021**, *253*. https://doi.org/10.1016/j.carbpol.2020.117277.

(8) Sagnelli, D.; Cavanagh, R.; Xu, J.; Swainson, S. M. E.; Blennow, A.; Duncan, J.; Taresco, V.; Howdle, S. Starch/Poly (Glycerol-Adipate) Nanocomposite Film as Novel Biocompatible Materials. *Coatings* **2019**, *9* (8). https://doi.org/10.3390/coatings9080482.

(9) Vestri, A.; Pearce, A. K.; Cavanagh, R.; Styliari, I. D.; Sanders, C.; Couturaud, B.; Schenone, S.; Taresco, V.; Jakobsen, R. R.; Howdle, S. M.; Musumeci, F.; Sagnelli, D. Starch/Poly(Glycerol-Adipate) Nanocomposites: A Novel Oral Drug Delivery Device. *Coatings* **2020**, *10* (2). https://doi.org/10.3390/coatings10020125.

(10) Belgacem, M. N.; Gandini, A. Monomers, Polymers and Composites from Renewable Resources. *Monomers, Polym. Compos. from Renew. Resour.* **2008**. https://doi.org/10.1016/B978-0-08-045316-3.X0001-4.

(11) Deng, Q.; Wang, Q.; Wang, Q.; Huang, Q.; Yin, P. Study on Saponification Technology of Waste Edible Oil. *3rd Int. Conf. Bioinforma. Biomed. Eng. iCBBE 2009* **2009**. https://doi.org/10.1109/ICBBE.2009.5163501.

(12) Rüdiger, A.; Hendil-Forssell, P.; Hedfors, C.; Martinelle, M.; Trey, S.; Johansson, M. Chemoenzymatic Route to Renewable Thermosets Based on a Suberin Monomer. *J. Renew. Mater.* **2013**, *1* (2), 124–140. https://doi.org/10.7569/JRM.2012.634109.

(13) Cordeiro, N.; Belgacem, N. M.; Gandini, A.; Neto, C. P. Cork Suberin as a New Source of

582 Chemicals: 2. Crystallinity, Thermal and Rheological Properties. *Bioresour. Technol.* **1998**, *63*
583 (2), 153–158. https://doi.org/10.1016/S0960-8524(97)00073-4.

584 (14) Ekman, R. The Suberin Monomers and Triterpenoids from the Outer Bark of Betula Verrucosa
585 Ehrh. *Holzforschung* **1983**, *37* (4), 205–211. https://doi.org/10.1515/hfsg.1983.37.4.205.

586 (15) Lulai, E. C. Demystifying Suberin. *Am. J. potato Res. an Off. Publ. Potato Assoc. Am.* **2018**, *95*
587 (4), 227–240. https://doi.org/10.1007/BF02851647.

588 (16) Campanella, A.; Baltanás, M. A.; Capel-Sánchez, M. C.; Campos-Martín, J. M.; Fierro, J. L. G.
589 Soybean Oil Epoxidation with Hydrogen Peroxide Using an Amorphous Ti/SiO2 Catalyst. *Green*
590 *Chem.* **2004**, *6* (7), 330–334. https://doi.org/10.1039/b404975f.

591 (17) Anuar, S. T.; Zhao, Y. Y.; Mugo, S. M.; Curtis, J. M. Studies on the Epoxidation of Mahua Oil
592 (Madhumica Indica) by Hydrogen Peroxide. *J. Am. Oil Chem. Soc.* **2012**, *89* (11), 1365–1371.
593 https://doi.org/10.1080/03602559.2010.512338.

594 (18) Ortiz, P.; Vendamme, R.; Eevers, W. Fully Biobased Epoxy Resins from Fatty Acids and Lignin.
595 *Molecules* **2020**, *25* (5), 1–11. https://doi.org/10.3390/molecules25051158.

596 (19) Torron, S.; Semlitsch, S.; Martinelle, M.; Johansson, M. Biocatalytic Synthesis of Epoxy Resins
597 from Fatty Acids as a Versatile Route for the Formation of Polymer Thermosets with Tunable
598 Properties. *Biomacromolecules* **2016**, *17* (12), 4003–4010.
599 https://doi.org/10.1021/acs.biomac.6b01383.

600 (20) Noè C., Malburet S., Bouvet-Marchand A., Grailot A., Loubat C., S. M. Cationic
601 Photopolymerization of Bio-Renewable Epoxidized Monomers. *Prog. Org. Coatings* **2019**, *133*,
602 131–138.

(21) Douliez, J. P.; Barrault, J.; Jerome, F.; Heredia, A.; Navailles, L.; Nallet, F. Glycerol Derivatives of Cutin and Suberin Monomers: Synthesis and Self-Assembly. *Biomacromolecules* **2005**, *6* (1), 30–34. https://doi.org/10.1021/bm049325o.

(22) Sousa, A. F.; Silvestre, A. J. D.; Gandini, A.; Neto, C. P. Synthesis of Aliphatic Suberin-like Polyesters by Ecofriendly Catalytic Systems. *High Perform. Polym.* **2012**, *24* (1), 4–8. https://doi.org/10.1177/0954008311431114.

(23) Sousa, A. F.; Gandini, A.; Silvestre, A. J. D.; Neto, C. P.; Cruz Pinto, J. J. C.; Eckerman, C.; Holmbom, B. Novel Suberin-Based Biopolyesters: From Synthesis to Properties. *J. Polym. Sci. Part A Polym. Chem.* **2011**, *49* (10), 2281–2291. https://doi.org/10.1002/pola.24661.

(24) Sousa, A. F.; Gandini, A.; Silvestre, A. J. D.; Pascoal Neto, C. Synthesis and Characterization of Novel Biopolyesters from Suberin and Model Comonomers. *ChemSusChem* **2008**, *1* (12), 1020–1025. https://doi.org/10.1002/cssc.200800178.

(25) Semlitsch, S.; Torron, S.; Johansson, M.; Martinelle, M. Enzymatic Catalysis as a Versatile Tool for the Synthesis of Multifunctional, Bio-Based Oligoester Resins. *Green Chem.* **2016**, *18* (7), 1923–1929. https://doi.org/10.1039/c5gc02597d.

(26) Torron, S.; Johansson, M. Oxetane-Terminated Telechelic Epoxy-Functional Polyesters as Cationically Polymerizable Thermoset Resins: Tuning the Reactivity with Structural Design. *J. Polym. Sci. Part A Polym. Chem.* **2015**, *53* (19), 2258–2266. https://doi.org/10.1002/pola.27673.

(27) Tsioptsias, C.; Paraskevopoulos, M. K.; Christofilos, D.; Andrieux, P.; Panayiotou, C. Polymeric Hydrogels and Supercritical Fluids: The Mechanism of Hydrogel Foaming. *Polymer (Guildf).* **2011**, *52* (13), 2819–2826. https://doi.org/10.1016/j.polymer.2011.04.043.

(28) Gutiérrez, C.; Garcia, M. T.; Curia, S.; Howdle, S. M.; Rodriguez, J. F. The Effect of CO2 on the Viscosity of Polystyrene/Limonene Solutions. *J. Supercrit. Fluids* **2014**, *88*, 26–37. https://doi.org/10.1016/j.supflu.2014.01.012.

(29) Picchioni, F. Supercritical Carbon Dioxide and Polymers: An Interplay of Science and Technology. *Polym. Int.* **2014**, *63* (8), 1394–1399. https://doi.org/10.1002/pi.4722.

(30) Baheti, P.; Gimello, O.; Bouilhac, C.; Lacroix-Desmazes, P.; Howdle, S. M. Sustainable Synthesis and Precise Characterisation of Bio-Based Star Polycaprolactone Synthesised with a Metal Catalyst and with Lipase. *Polym. Chem.* **2018**, *9* (47), 5594–5607. https://doi.org/10.1039/c8py01266k.

(31) J. Jennings, M. Beija, A.P. Richez, S.D. Cooper, P.E. Mignot, K.J. Thurecht, K.S. Jack, S. M. H. One- Pot Synthesis of Block Copolymers in Supercritical Carbon Dioxide: A Simple Versatile Route to Nanostructured Microparticles. *J. Am. Chem. Soc.* **2012**, No. 134, 4772–4781.

(32) Tsivintzelis, I.; Pavlidou, E.; Panayiotou, C. Biodegradable Polymer Foams Prepared with Supercritical CO2-Ethanol Mixtures as Blowing Agents. *J. Supercrit. Fluids* **2007**, *42* (2), 265–272. https://doi.org/10.1016/j.supflu.2007.02.009.

(33) Winters, M. A.; Knutson, B. L.; Debenedetti, P. G.; Sparks, H. G.; Przybycien, T. M.; Stevenson, C. L.; Prestrelski, S. J. Precipitation of Proteins in Supercritical Carbon Dioxide. *J. Pharm. Sci.* **1996**, *85* (6), 586–594. https://doi.org/10.1021/js950482q.

(34) Bungert, B.; Sadowski, G.; Arlt, W. Supercritical Antisolvent Fractionation: Measurements in the Systems Monodisperse and Bidisperse Polystyrenecyclohexanecarbon Dioxide. *Fluid Phase Equilib.* **1997**, *139* (1–2), 349–359. https://doi.org/10.1016/S0378-3812(97)00167-2.

(35) Mendes, R. L.; Nobre, B. P.; Cardoso, M. T.; Pereira, A. P.; Palavra, A. F. Supercritical Carbon Dioxide Extraction of Compounds with Pharmaceutical Importance from Microalgae. *Inorganica Chim. Acta* **2003**, *356*, 328–334. https://doi.org/10.1016/S0020-1693(03)00363-3.

(36) Howdle, S. M.; Watson, M. S.; Whitaker, M. J.; Popov, V. K.; Davies, M. C.; Mandel, F. S.; Wang, J. D.; Shakesheff, K. M. Supercritical Fluid Mixing: Preparation of Thermally Sensitive Polymer Composites Containing Bioactive Materials. *Chem. Commun.* **2001**, No. 1, 109–110. https://doi.org/10.1039/b008188o.

(37) Jessop, P. G.; Leitner, W. Supercritical Fluids as Media for Chemical Reactions. *Chemical Synthesis Using Supercritical Fluids*. July 8, 1999, pp 1–36. https://doi.org/doi:10.1002/9783527613687.ch1.

(38) Cooper, A. I. Polymer Synthesis and Processing Using Supercritical Carbon Dioxide. *J. Mater. Chem.* **2000**, *10* (2), 207–234. https://doi.org/10.1039/a906486i.

(39) Gourgouillon, D.; Avelino, H. M. N. T.; Fareleira, J. M. N. A.; Nunes da Ponte, M. Simultaneous Viscosity and Density Measurement of Supercritical CO2-Saturated PEG 400. *J. Supercrit. Fluids* **1998**, *13* (1–3), 177–185. https://doi.org/10.1016/S0896-8446(98)00050-3.

(40) Royer, J. R.; DeSimone, J. M.; Khan, S. A. High-Pressure Rheology and Viscoelastic Scaling Predictions of Polymer Melts Containing Liquid and Supercritical Carbon Dioxide. *J. Polym. Sci. Part B Polym. Phys.* **2001**, *39* (23), 3055–3066. https://doi.org/10.1002/polb.10057.

(41) C. Loeker, F.; J. Duxbury, C.; Kumar, R.; Gao, W.; A. Gross, R.; M. Howdle, S. Enzyme-Catalyzed Ring-Opening Polymerization of ε-Caprolactone in Supercritical Carbon Dioxide. *Macromolecules* **2004**, *37* (7), 2450–2453. https://doi.org/10.1021/ma0349884.

(42) Lepilleur, C.; J. Beckman, E. Dispersion Polymerization of Methyl Methacrylate in Supercritical CO2. *Macromolecules* **1997**, *30* (4), 745–756. https://doi.org/10.1021/ma960764s.

(43) L. O'Neill, M.; Z. Yates, M.; P. Johnston, K.; D. Smith, C.; P. Wilkinson, S. Dispersion Polymerization in Supercritical CO2 with a Siloxane-Based Macromonomer: 1. The Particle Growth Regime. *Macromolecules* **1998**, *31* (9), 2838–2847. https://doi.org/10.1021/ma971314i.

(44) Ferdosian, F.; Yuan, Z.; Anderson, M.; Xu, C. Sustainable Lignin-Based Epoxy Resins Cured with Aromatic and Aliphatic Amine Curing Agents: Curing Kinetics and Thermal Properties. *Thermochim. Acta* **2015**, *618*, 48–55. https://doi.org/10.1016/j.tca.2015.09.012.

(45) O'Brien, D. M.; Vallieres, C.; Alexander, C.; Howdle, S. M.; Stockman, R. A.; Avery, S. V. Epoxy-Amine Oligomers from Terpenes with Applications in Synergistic Antifungal Treatments. *J. Mater. Chem. B* **2019**, *7* (34), 5222–5229. https://doi.org/10.1039/c9tb00878k.

(46) Nameer, S.; Johansson, M. Fully Bio-Based Aliphatic Thermoset Polyesters via Self-Catalyzed Self-Condensation of Multifunctional Epoxy Monomers Directly Extracted from Natural Sources. *J. Coatings Technol. Res.* **2017**, *14* (4), 757–765. https://doi.org/10.1007/s11998-017-9920-y.

(47) Haddleton, A. J.; Bassett, S. P.; Howdle, S. M. Comparison of Polymeric Particles Synthesised Using ScCO2 as the Reaction Medium on the Millilitre and Litre Scale. *J. Supercrit. Fluids* **2020**, *160*. https://doi.org/10.1016/j.supflu.2020.104785.

(48) Schneider, C. A.; Rasband, W. S.; Eliceiri, K. W. NIH Image to ImageJ: 25 Years of Image Analysis. *Nat. Methods* **2012**, *9* (7), 671–675. https://doi.org/10.1038/nmeth.2089.

(49) Curia, S.; Barclay, A. F.; Torron, S.; Johansson, M.; Howdle, S. M. Green Process for Green Materials: Viable Low-Temperature Lipase-Catalysed Synthesis of Renewable Telechelics in

687 Supercritical CO2. *Philos. Trans. R. Soc. A Math. Phys. Eng. Sci.* **2015**, *373* (2057).
688 https://doi.org/10.1098/rsta.2015.0073.

689 (50) Marty, A.; Chulalaksananukul, W.; Willemot, R. M.; Condoret, J. S. Kinetics of Lipase-catalyzed
690 Esterification in Supercritical CO2. *Biotechnol. Bioeng.* **1992**, *39* (3), 273–280.
691 https://doi.org/10.1002/bit.260390304.

692 (51) D'Almeida Gameiro, M.; Goddard, A.; Taresco, V.; Howdle, S. M. Enzymatic One-Pot Synthesis
693 of Renewable and Biodegradable Surfactants in Supercritical Carbon Dioxide (ScCO2). *Green*
694 *Chem.* **2020**, *22* (4), 1308–1318. https://doi.org/10.1039/c9gc04011k.

695 (52) Curia, S.; Howdle, S. M. Towards Sustainable Polymeric Nano-Carriers and Surfactants: Facile
696 Low Temperature Enzymatic Synthesis of Bio-Based Amphiphilic Copolymers in ScCO2. *Polym.*
697 *Chem.* **2016**, *7* (11), 2130–2142. https://doi.org/10.1039/c6py00066e.

698 (53) Natta, G.; Pasquon, I.; Zambelli, A.; Gatti, G. Dependence of the Melting Point of Isotactic
699 Polypropylenes on Their Molecular Weight and Degree of Stereospecificity of Different Catalytic
700 Systems. *Makromol. Chem.* **1964**, *70*, 191.

701 (54) Hintermeyer, J.; Herrmann, A.; Kahlau, R.; Goiceanu, C.; Rössler E, E. A. Molecular Weight
702 Dependence of Glassy Dynamics in Linear Polymers Revisited. *Macromolecules* **2008**, *41* (23),
703 9335–9344. https://doi.org/10.1021/ma8016794.

704 (55) Hong, S. G.; Hsu, H. W.; Ye, M. T. Thermal Properties and Applications of Low Molecular
705 Weight Polyhydroxybutyrate. *J. Therm. Anal. Calorim.* **2013**, *111* (2), 1243–1250.
706 https://doi.org/10.1007/s10973-012-2503-3.

707 (56) Menager, C.; Guigo, N.; Vincent, L.; Sbirrazzuoli, N. Polymerization Kinetic Pathways of

Epoxidized Linseed Oil with Aliphatic Bio-based Dicarboxylic Acids. *J. Polym. Sci.* **2020**. https://doi.org/10.1002/pol.20200118.

(57) González, M. G.; Cabanelas, J. C.; Baselga, J. Applications of FTIR on Epoxy Resins - Identification, Monitoring the Curing Process, Phase Separation and Water Uptake. *Infrared Spectrosc. - Mater. Sci. Eng. Technol.* **2012**. https://doi.org/10.5772/36323.

(58) Menard, K. P. Dynamic Mechanical Analysis: A Practical Introduction, Second Edition. **2008**, 240.

(59) Stutz, H.; Illers, K. -H; Mertes, J. A Generalized Theory for the Glass Transition Temperature of Crosslinked and Uncrosslinked Polymers. *J. Polym. Sci. Part B Polym. Phys.* **1990**, *28* (9), 1483–1498. https://doi.org/10.1002/polb.1990.090280906.

(60) Lesser, A. J.; Crawford, E. The Role of Network Architecture on the Glass Transition Temperature of Epoxy Resins. *J. Appl. Polym. Sci.* **1997**, *66* (2), 387–395. https://doi.org/10.1002/(sici)1097-4628(19971010)66:2<387::aid-app19>3.0.co;2-v.

(61) Schreck, K. M.; Leung, D.; Bowman, C. N. Hybrid Organic/Inorganic Thiol-Ene-Based Photopolymerized Networks. *Macromolecules* **2011**, *44* (19), 7520–7529. https://doi.org/10.1021/ma201695x.

(62) Wang, Y.; Liu, W.; Qiu, Y.; Wei, Y. A One-Component, Fast-Cure, and Economical Epoxy Resin System Suitable for Liquid Molding of Automotive Composite Parts. *Materials (Basel).* **2018**, *11* (5). https://doi.org/10.3390/ma11050685.

(63) Liu, R.; Xu, Y.; Wang, L.; Zhang, F.; Chen, P.; Li, Y.; Chen, Y. Visible Light-Induced Cationic Photopolymerization by Diphenyliodonium Hexafluorophosphate and Benzothiadiazole Dyes.

729 *Polym. Bull.* **2020**. https://doi.org/10.1007/s00289-020-03345-7.

730 (64) Kishi, H.; Fujita, A.; Miyazaki, H.; Matsuda, S.; Murakami, A. Synthesis of Wood-Based Epoxy
731 Resins and Their Mechanical and Adhesive Properties. *J. Appl. Polym. Sci.* **2006**, *102* (3), 2285–
732 2292. https://doi.org/10.1002/app.24433.

733 (65) Nayak, A. K.; Das, B. Introduction to Polymeric Gels. *Polym. Gels* **2018**, 3–27.
734 https://doi.org/10.1016/b978-0-08-102179-8.00001-6.

735 (66) España, L.; Heredia-Guerrero, J. A.; Segado, P.; Benítez, J. J.; Heredia, A.; Domínguez, E.
736 Biomechanical Properties of the Tomato (Solanum Lycopersicum) Fruit Cuticle during
737 Development Are Modulated by Changes in the Relative Amounts of Its Components. *New Phytol.*
738 **2014**, *202* (3), 790–802. https://doi.org/10.1111/nph.12727.

739 (67) Ahn, B. J. K.; Kraft, S.; Sun, X. S. Solvent-Free Acid-Catalyzed Ring-Opening of Epoxidized
740 Oleochemicals Using Stearates/Stearic Acid, and Its Applications. *J. Agric. Food Chem.* **2012**, *60*
741 (9), 2179–2189. https://doi.org/10.1021/jf204275q.

742 (68) Altuna, F. I.; Pettarin, V.; Williams, R. J. J. Self-Healable Polymer Networks Based on the Cross-
743 Linking of Epoxidised Soybean Oil by an Aqueous Citric Acid Solution. *Green Chem.* **2013**, *15*
744 (12), 3360–3366. https://doi.org/10.1039/c3gc41384e.

745